NASA CONTRACTOR REPORT

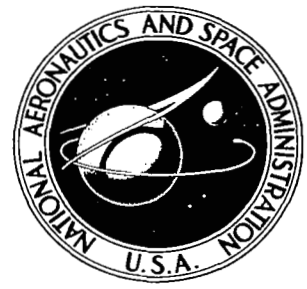

NASA CR-393

CATALYSIS OF HYDROGEN-ATOM RECOMBINATION IN ROCKET NOZZLES

by J. A. Lordi and R. E. Mates

Prepared under Contract No. NASr-109 *by*
CORNELL AERONAUTICAL LABORATORY, INC.
Buffalo, N. Y.
for

NATIONAL AERONAUTICS AND SPACE ADMINISTRATION • WASHINGTON, D. C. • MARCH 1966

NASA CR-393

CATALYSIS OF HYDROGEN-ATOM RECOMBINATION IN ROCKET NOZZLES

By J. A. Lordi and R. E. Mates

Prepared under Contract No. NASr-109 by
CORNELL AERONAUTICAL LABORATORY, INC.
Buffalo, N. Y.

for

NATIONAL AERONAUTICS AND SPACE ADMINISTRATION

For sale by the Clearinghouse for Federal Scientific and Technical Information
Springfield, Virginia 22151 – Price $2.00

ABSTRACT

The use of gas-phase catalysis has previously been suggested as a means of enhancing hydrogen-atom recombination and hence the performance of nuclear or electrically powered rocket engines. In an earlier study the use of carbon addition was examined by obtaining numerical solutions for nonequilibrium expansions of carbon-seeded hydrogen. In the present study the use of oxygen and an oxygen-nitrogen mixture as catalysts has been examined. The results of the calculations indicate, as do earlier solutions using carbon addition, that gas-phase catalysis leads to a marginal increase in specific impulse. In both instances hydrogen-atom recombination was significantly enhanced, but the accompanying increase in the molecular weight of the fluid led to slight losses or gains in specific impulse depending on the reaction-rate constants employed for the catalytic mechanisms.

Both the results of the present studies and those of the hydrogen-carbon system are used to establish the minimum requirements which an additive must satisfy to yield a gain in specific impulse. An expression is derived for a "catalytic parameter" which gives an approximation for the gain in performance which can be expected for a given additive. Also, the results of both studies show that a significant saving in tankage weight may be possible despite only marginal gains in specific impulse.

TABLE OF CONTENTS

1. INTRODUCTION

The high specific impulse available in low-thrust rocket-nozzle flows of dissociated hydrogen[1] can be severely penalized by departure from chemical equilibrium in the nozzle expansion.[2] Figure 1, taken from Ref. 2, demonstrates this nonequilibrium effect for reservoir conditions applicable to nuclear-heated or arc-heated rocket engines. The use of gas-phase catalysis of hydrogen-atom recombination has been suggested as a means of counteracting recombination losses.[3-5] Previously, exact numerical solutions were obtained for carbon-seeded hydrogen nozzle flows in order to examine the use of carbon as an additive.[3] The purpose of this report is to describe the results of a similar study on the use of oxygen and an oxygen-nitrogen mixture as additives. Oxygen and an oxygen-nitrogen mixture were selected in an attempt to improve the marginal gains in specific impulse found from the hydrogen-carbon calculations.

Gas-phase catalysis provides alternative paths for hydrogen-atom recombination which are less susceptible to the phenomenon of "nozzle-flow freezing" than the termolecular path.

$$H + H + M \overset{k_{f_1}}{\rightleftharpoons} H_2 + M \qquad (1)$$

Letting R denote any chemical species, the alternative paths are of the form

$$H + R \overset{k_{f_2}}{\rightleftharpoons} RH \qquad (2)$$

$$H + RH \overset{k_{f_3}}{\rightleftharpoons} R + H_2 \qquad (3)$$

In order to yield a gain in specific impulse the degree to which hydrogen-atom recombination is enhanced by the above reaction mechanism must be sufficient to overcome the increase in molecular weight inherent in adding any component to hydrogen. This fact may be seen from the following relation for the infinite-expansion, equilibrium-flow specific impulse

$$I_\infty = \frac{\sqrt{2H_o}}{g} = \frac{1}{g}\left(\frac{2}{m_o}\sum_{j=1}^{s} X_{j_o} h_{j_o}\right)^{1/2} \qquad (4)$$

where H_o is the specific reservoir enthalpy, g the acceleration of gravity, X_j the mole-fraction of each species in the mixture, h_j the molar enthalpy of each species, and m_o the reservoir molecular weight. The molecular-weight penalty, i. e. the increase in m_o , depends on the kind and amount of additive.

Before describing the recent nozzle-flow solutions for the hydrogen-oxygen and hydrogen-oxygen-nitrogen systems, the results of the earlier study of the hydrogen-carbon system are reviewed. Then the formulation of chemical-kinetic models for the hydrogen-oxygen and hydrogen-oxygen-nitrogen systems is described. The results of a literature search for reaction-rate data for these systems are included in the discussion of the computational models. Next the results of the nozzle flow solutions for hydrogen with these two additives are presented and their application to upper-stage rocket engines is discussed. It is shown that additives can be effective in saving tankage weight. Also, the implications of the gas-phase catalysis studies to date, as they concern other additives, are described in the form of criteria which must be satisfied if a given additive is to improve the performance of a hydrogen rocket engine.

2. REVIEW OF RESULTS OF HYDROGEN-CARBON GAS-PHASE CATALYSIS STUDIES

In the initial studies of catalysis of hydrogen-atom recombination,[3] carbon was chosen as an additive because of its ability to form hydrogenous compounds and hence to provide alternative paths of the form (2) and (3). In the solutions obtained for carbon-seeded hydrogen nozzle flows the dominant bimolecular path for hydrogen-atom recombination was found to be the reaction in which RH in Eq. (2) represents acetylene (C_2H_2).

As discussed in Ref. 3, a model consisting of 8 species and 12 reactions was found to adequately describe the hydrogen-carbon nozzle flows at the conditions of interest. The rate constants for the bimolecular reactions included in the model were estimated on the basis of low-temperature experiments and simple chemical-kinetic calculations. The rate constants were written in the form

$$k_f = P z e^{-E/R_o T} \tag{5}$$

where P is the steric factor, z the collision frequency, and E the activation energy. The nozzle flow calculations were performed assuming two values, an order of magnitude different, for the steric factors. The steric factors used in the acetylene reaction were 10^{-2} and 10^{-1} which bracket expected values based on estimates and low-temperature data.

In the range of reservoir conditions treated in Ref. 3 ($3500°K \leq T_o \leq 4500°K$, $0.1 \text{ atm} \leq p_o \leq 10.0 \text{ atm}$), the calculations showed a slight loss in specific impulse relative to the pure-hydrogen, nonequilibrium solution when the lower estimate was used for the bimolecular

rate constants. When the higher estimates for these rates were used, the recombination of hydrogen atoms was increased enough to overcome the molecular weight penalty and yield a net gain in nozzle performance.

For reservoir conditions of 4500°K and 10 atm, solutions were obtained for a wide range of carbon-hydrogen mixture ratios using the higher bimolecular rate constants. An optimum mixture ratio was found to exist due to the opposing effects of the molecular-weight penalty and catalysis. For the above reservoir state a maximum impulse gain of 100 sec relative to a pure-hydrogen value of 1500 sec was found for a carbon to hydrogen atom ratio of about .01.

Another finding in the hydrogen-carbon studies was that the gasdynamic and important chemical-kinetic properties of the nozzle flow could be calculated using a 4-species, 4-reaction chemical-kinetic model in the computer program. The species included in the calculation were H_2, H, C_2H and C_2H_2. The reactions included were two termolecular-recombination paths and the two step path (2) and (3) with R corresponding to C_2H. In one of the termolecular paths H-atom was the third body and in the other all of the remaining species were treated as equally efficient third bodies. Using this simple model, the results obtained for the specific impulse and for the H_2 and H concentrations agreed to within 1% with the results obtained using the 8-species, 12-reaction model. The C_2H and C_2H_2 concentrations were typically overestimated by about 50% as a result of lumping all the carbon content in these two species. Using this model, which preserves the salient features of the hydrogen-carbon nozzle flows, greatly reduces the machine computing time required for a solution.

3. FORMULATION OF CHEMICAL-KINETIC MODELS FOR HYDROGEN-OXYGEN AND HYDROGEN-OXYGEN-NITROGEN SYSTEMS

As discussed in the Introduction, the use of oxygen and oxygen-nitrogen additives in hydrogen nozzle flows is aimed at providing alternative paths similar to (2) and (3) for hydrogen-atom recombination. In this section the formulation of the chemical-kinetic models employed in obtaining nozzle-flow solutions is described. First, the selection procedure for the important species is discussed. Then presented are the results of a literature survey of experimental rate-constant data for reactions among the species in the models. Finally, the determination of the kinetically important reactions and the final truncation of the models are discussed.

3.1 Species Included in the Computational Models

Hydrogen-Oxygen System

Preliminary calculations were carried out in order to determine the important species in the hydrogen-oxygen system. The species assumed to be present were H_2, O_2, H, O, OH, H_2O, HO_2, H_2O_2 and O_3. The thermodynamic data for H_2, O_2, H, O, OH and H_2O were taken from Ref. 6 and that for HO_2, H_2O_2 and O_3 from Ref. 7. Equilibrium compositions were computed at temperatures of 3000 and 4500°K, pressures of 1 and 10 atm and O/H atom ratios of .01 and .001. These calculations showed negligible amounts of HO_2, H_2O_2 and O_3, in all cases more than 7 orders of magnitude smaller than the dominant species, hydrogen atom. If the nozzle flow were to remain in chemical equilibrium then these species would be formed as the gas expanded to lower temperature. However, chemical freezing is expected at about the throat temperature and hence these species will not become kinetically or energetically important. Consequently, these three

species were not included in the kinetic model. The remaining species, as will be seen in the ensuing section, participate in reactions which provide possible alternative paths for hydrogen-atom recombination.

Hydrogen-Oxygen-Nitrogen System

In the discussion of Ref. 3, the addition of an oxygen-nitrogen mixture to catalyze hydrogen-atom recombination was suggested by Sugden on the basis of flame studies.[8] The addition of nitrogen to hydrogen and oxygen lends the possibility of a catalytic path (Eqs. (2) and (3)) with HNO as an intermediate. Equilibrium calculations were also done to determine the significant chemical species present in the hydrogen-oxygen-nitrogen system. The temperature and pressure chosen were 4500°K and 10 atm with O/N/H atom ratios of 10/1/1000, 5/5/1000, 1/10/1000, 10/1/10,000, 5/5/10,000 and 1/10/10,000. The species assumed present were H_2, O_2, H, O, OH, H_2O, N_2, N, NO, HNO, HO_2, H_2O_2, O_3, NO_2, N_2O. Again the thermodynamic data were taken from Refs. 6 and 7. The concentrations of the following species were found to be negligible: HO_2, H_2O_2, O_3, NO_2, N_2O.

3.2 Rate Constant Data for Hydrogen-Oxygen-Nitrogen Reactions

In this section the rates of reactions among the species included in the kinetic models are investigated. These reactions and the selected values of the rate constants are listed in Table 1. As evident from Ref. 9, which presents a comprehensive survey of rate constants reported for H-O-N reactions, there is considerable uncertainty in these data. The rates chosen for the calculations are those that appear from the literature to be best substantiated. In some cases the selection, by necessity, is

somewhat arbitrary. Because of these uncertainties it was felt necessary to assess the corresponding uncertainty in the final results. In addition to the calculations based on the selected rates, calculations were carried out using the largest reported rates, which are listed in parentheses.

Reactions marked with an asterisk (*) were subsequently found, in the numerical calculations, to be kinetically unimportant. Forward rates were used for the reactions as written, with reverse rates calculated from the equilibrium constants.

As noted in Table 1, the average values of the data reported for reactions 1, 2, 6, 7, 10 were selected for use in the computations. The values reported for reactions 1, 2 and 6 varied by an order of magnitude while those reported for 7 and 10 varied by two orders of magnitude. Also, the highest of the reported values were selected for reactions 3, 4, 8, 13, 14 and 16 because they appeared to be the most reliable.

The mechanism for the catalysis of H-atom recombination through the intermediate HNO is not firmly established. The two sets of experimental results which have been published are somewhat contradictory. Flame studies[8] at 1600-2000°K indicate that reactions 18 and 19 are the rate controlling steps, with reaction 17 maintained essentially in equilibrium. Lower temperature (300°K) experiments in a flow system[22] show reaction 18 to be very fast compared to the reverse of 17, with a steady state concentration of HNO maintained by reaction 17. In the present calculations the value of $k_{f_{17}}$ reported in Ref. 22 is used. The value of $k_{f_{18}}$ is taken from Ref. 8 and $k_{f_{19}}$ is taken as $15 k_{f_{18}}$, as suggested in Ref. 8.

3.3 Final Truncation of Kinetic Models

Hydrogen-Oxygen System

To assess the relative importance of individual reactions in the kinetic mechanism, a nonequilibrium, nozzle-expansion calculation was made from reservoir conditions of 4500°K and 10 atm, including reactions 1 through 11 and the species found to be dominant from the equilibrium calculations of Sec. 3.1 (H_2, O_2, H, O, OH, H_2O). In the nozzle-flow computer program the species conservation equations are written

$$\frac{d\gamma_j}{dx} = \sum_i \frac{Q_{ij}}{\rho u} \tag{6}$$

where γ_j is the concentration of the j^{th} species in moles/gm, x the distance along the nozzle, and Q_{ij} is the number of moles of the j^{th} species produced per unit volume per unit time by the i^{th} reaction.

$$Q_{ij} = \left(\nu'_{ij} - \nu_{ij}\right)\left[k_{f_i}\prod_{j=1}^{s}(\rho\gamma_j)^{\nu_{ij}} - \frac{k_{f_i}}{K_i}\prod_{j=1}^{s}(\rho\gamma_j)^{\nu'_{ij}}\right] \tag{7}$$

where ν'_{ij} and ν_{ij} are the stoichiometric coefficients of the j^{th} species on the product and reactant side respectively of the i^{th} reaction. The results obtained for $Q_{ij} / \rho u \left(\nu'_{ij} - \nu_{ij}\right)$ in the above-mentioned calculation are shown in Table 2 for various area ratios in the nozzle. As can be seen from Table 2, reactions 6, 9, 10 contribute little to the over-all kinetics, and thus these reactions and the species O_2 were deleted from the model. The calculation was repeated and showed negligible variation in concentrations of the species retained.

The model used in obtaining the results discussed in this report, then, consisted of species H_2, H, O, OH, H_2O and reactions 1-5, 7, 8, 11.

Hydrogen-Oxygen-Nitrogen System

Reactions 1-19 were considered in the preliminary kinetic calculations. The first few steps of a nonequilibrium, nozzle-flow solution were computed, and, as before, the individual rates were compared. Examination showed that reactions 9, 10, 12, 13 made a negligible contribution.

The final model for the hydrogen-oxygen-nitrogen system consisted of species H_2, O_2, H, O, OH, H_2O, N_2, N, NO, HNO and reactions 1-8, 11, 14-19.

4. RESULTS FOR SPECIFIC IMPULSE IN NOZZLE FLOWS OF HYDROGEN WITH OXYGEN AND OXYGEN-NITROGEN ADDITION

In this section the results of numerical solutions for nozzle flows of hydrogen with oxygen and oxygen-nitrogen addition are presented. In all of these solutions the truncated chemical kinetic models described in the previous section were employed. Also the nozzle geometry specified for all solutions is a hyperbolic, axisymmetric shape which becomes conical at large area ratios.

$$A/A^* = 1.0 + \left(\frac{x \tan\theta}{r^*}\right)^2 \tag{8}$$

where r^* is the throat radius, θ is half-angle of the asymptote cone, and x is the axial distance with the origin at the throat. For the present case $r^*/\tan\theta$ was taken to be 1 cm.

The solutions were obtained using a computer program developed at CAL for the numerical integration of one-dimensional, inviscid expansions of multicomponent mixtures undergoing coupled chemical reactions.[24] In this type of calculation, numerical inaccuracies which can lead to unstable solutions are encountered when integrating the species conservation equations where the species are near a local-equilibrium value. The procedure of adding fast, alternative paths for hydrogen-atom recombination, if successful, leads to such difficulties. The method by which these difficulties have been resolved in the CAL nozzle-flow computer program is discussed in Ref. 25.

4.1 Hydrogen-Oxygen System

Solutions were obtained for an oxygen-to-hydrogen atom ratio of .01 and reservoir conditions of 4500°K, 10 atm. The resulting values for the

final or frozen hydrogen-atom concentration and the infinite-expansion specific impulse are shown in Table 3. Recall that the final kinetic model consists of the species H_2, H, O, OH, and H_2O and reactions 1-5, 7, 8 and 11. Results are shown in Table 3 using both the preferred and highest values of the rate constants for reactions 7 and 11 (see Table 1). Both the pure hydrogen and hydrogen-carbon results corresponding to this mixture ratio and reservoir condition are also shown in Table 3. In the earlier gas-phase catalysis studies, the relative gain or loss in the infinite-expansion value of specific impulse was shown to accurately reflect the percentage gain or loss at finite area ratios.

As may be seen from Table 3, when the preferred values of the experimental rate data are employed in the hydrogen-oxygen nozzle-flow calculations, a loss in impulse results. Notice, however, that the frozen concentration of hydrogen atoms is lower for the hydrogen-oxygen than for the pure-hydrogen system. This behavior indicates that hydrogen-atom recombination is being catalyzed, but not enough to overcome the molecular weight penalty due to oxygen addition. A similar failure to overcome the molecular weight penalty was encountered in the hydrogen-carbon studies when the lower estimates for the bimolecular rate constants were used (see Table 3).

The variation of the species concentrations for this case are shown in Fig. 2. These species distributions were obtained using the preferred values of the reaction-rate constants listed in Table 1. The equilibrium-flow variations of the species concentrations are included in Fig. 2 for comparison. As can be seen from this graph the flow composition departs

from equilibrium as the flow expands and the hydrogen-atom concentration freezes. The asymptotic, frozen value of the hydrogen-atom concentration in the corresponding pure-hydrogen expansion is also shown on Fig. 2 and clearly indicates that, despite the net loss in performance, hydrogen-atom recombination is being catalyzed.

When the upper limits of the range of experimental rate-constant data are used for the reactions involving hydrogen- and oxygen-bearing species, a slight gain over the pure-hydrogen impulse is obtained for the conditions illustrated in Table 3. As can be seen from Table 3 the effect on specific impulse of increasing the rates of the catalytic mechanism is about the same for the hydrogen-oxygen and hydrogen-carbon systems. On the basis of the estimates for the reaction-rate constants employed to obtain the results in Table 3, carbon addition appears to be slightly more successful than oxygen addition.

An important difference between the hydrogen-oxygen and hydrogen-carbon systems is in the catalytic mechanism. As discussed in Sec. 2, the alternative path to the termolecular hydrogen-atom recombination in the hydrogen-carbon system involves two bimolecular reaction steps (Eqs. (2) and (3)). From the nozzle-flow solutions for the hydrogen-oxygen system the following reactions were found to be the dominant paths for hydrogen-atom recombination.

$$\begin{aligned} H + OH + M &\rightleftharpoons H_2O + M \\ H + H_2O &\rightleftharpoons OH + H_2 \end{aligned} \qquad (9)$$

$$H + O + M \rightleftharpoons OH + M$$
$$H + OH \rightleftharpoons O + H_2 \qquad (10)$$

Although the first step of these reactions is termolecular, the rate of consumption of hydrogen atoms is greater via these mechanisms than by direct termolecular recombination.

In Table 4 the numerical results for the contribution of individual reactions in the kinetic model to the hydrogen-atom gradient are shown at several area ratios. The two cases shown correspond to the two hydrogen-oxygen results presented in Table 3. As can be seen from Table 4, when the mean values of the rate constants are used for reactions 7 and 11 the dominant path for the removal of hydrogen atoms is the mechanism represented by Eq. (9). At higher area ratios the second reaction in (9) (reaction 5 in Table 1) reverses direction and produces hydrogen atoms. However, at this point in the expansion, the over-all hydrogen-atom gradient is small and the concentration is essentially frozen (see Fig. 2). When the upper limit of the experimental rate-constant data is used for reactions 7 and 11, the mechanism represented by Eq. (10) is the dominant path for the removal of hydrogen atoms.

The effect of a change in reservoir pressure on the performance of the hydrogen-oxygen system is indicated in Table 5. Here, the hydrogen-oxygen results for T_o = 4500°K, p_o = 1 atm, the corresponding hydrogen-carbon results, and the results for both mixtures at T_o = 4500°K, p_o = 10 atm are compared. The highest values of the experimental rate constants are used in this comparison. The results in this table indicate that while

the gain in performance realized in the hydrogen-oxygen flows increases when p_o is decreased from 10 atm to 1 atm, the improvement over the uncatalyzed hydrogen expansion is small for both reservoir pressures. The gain in performance obtained with carbon addition decreases slightly with this change in reservoir pressure, but is larger than the hydrogen-oxygen gain at both pressures. It should also be pointed out that the results of Fig. 1 indicate that the gains observed for these catalysts are small compared with the theoretically available gains.

As noted in Sec. 2, in the earlier gas-phase catalysis studies the existence of an optimum mixture ratio for the hydrogen-carbon system was found. For reservoir conditions of 4500°K and 10 atm the optimum C/H atom ratio was found to be about .01. At this optimum mixture ratio a gain in specific impulse of 100 sec in 1500 was obtained with the higher set of bimolecular reaction-rate constants. Nozzle flow solutions were obtained for several mixture ratios of hydrogen and oxygen at reservoir conditions of 4500°K and 10 atm. The results of these calculations, which were performed using the upper limit of the experimental rate constant data for reactions 7 and 11, are shown in Table 6.

The results of Table 6 also show the existence of an optimum mixture ratio. For this set of reservoir conditions the optimum mixture ratio for the hydrogen-oxygen system lies between .002 and .005. At lower mixture ratios the catalysis is limited due to insufficient additive. At higher mixture ratios the molecular-weight penalty overbalances the catalysis. This may be seen from the fact that at a mixture ratio of .05 the hydrogen-atom concentration is substantially lower than the pure hydrogen value, but so is

the specific impulse. It is difficult to predict the optimum mixture ratio at other reservoir conditions because it will be a complicated function of the molecular weight of the catalyst, the bond energy of the additive, and the rates of the catalytic mechanism.

4.2 Hydrogen-Oxygen-Nitrogen System

In Sec. 3 a computational model was formulated for the hydrogen-oxygen-nitrogen system. The model found to be appropriate to the nozzle-flow calculations consists of the species H_2, O_2, H, O, OH, H_2O, N_2, N, NO, HNO and reactions 1-8, 11, and 14-19 listed in Table 1. Using this chemical kinetic model, a nonequilibrium nozzle-flow solution has been obtained for $T_o = 4500°K$, $p_o = 10$ atm and mixture atom ratios of O/H = .005 and N/H = .005.

The results obtained for the hydrogen-atom concentration and nozzle specific impulse are the same as for the hydrogen-oxygen system having an O/H ratio of .01. As noted in the previous section a higher specific impulse was observed for the hydrogen-oxygen system for O/H = .005 than for O/H = .01. Thus, the addition of nitrogen to a mixture of oxygen with O/H = .005 led to no further catalysis of hydrogen-atom recombination, but reduced the specific impulse due to the molecular-weight penalty of the nitrogen. The reason that the additional path

$$\begin{aligned} H + NO + M &\rightleftharpoons HNO + M \\ H + HNO &\rightleftharpoons H_2 + NO \end{aligned} \qquad (11)$$

led to no further decrease in the hydrogen-atom concentration from the hydrogen-oxygen value is that the HNO decomposes at the reservoir condi-

tions of interest here. The numerical solution showed the NO and HNO concentrations at the nozzle throat to be respectively 2 and 4 orders of magnitude lower than the O, OH, and H_2O concentrations. These concentrations indicate that HNO and NO are not present in sufficient amounts for the mechanism (11) to consume hydrogen atoms as fast as the mechanisms given in Eqs. (9) and (10) unless the forward rates of (11) are much higher than the reported values. Thus, while the HNO mechanism for hydrogen-atom recombination is effective at flame temperatures (about 2000°K), it is not advantageous in high-temperature rocket nozzles.

5. DISCUSSION OF RESULTS

The results of the nozzle-flow calculations presented here and those presented earlier[3] indicate catalysis of hydrogen-atom recombination to be feasible. However, the gains are marginal within the uncertainty in the chemical-kinetic data for the catalytic mechanisms. Although the results obtained to date do not yield large performance gains, they may be employed to establish criteria to be satisfied by a successful additive. Furthermore, a marginal gain in impulse may still be important in upper-stage rocket engines due to an attendant reduction in tankage weight. These two items are discussed in detail in the following sections.

5.1 Criteria for Successful Catalysis of Hydrogen-Atom Recombination

In this section the implications of the results of the gas-phase catalysis studies for additives other than oxygen and carbon are discussed. As stated previously the reaction path to be catalyzed is

$$H + H + M \underset{k_{r_1}}{\overset{k_{f_1}}{\rightleftharpoons}} H_2 + M \qquad (1)$$

The suggestion is to provide the additional paths either of the form

$$H + R \underset{k_{r_2}}{\overset{k_{f_2}}{\rightleftharpoons}} RH \qquad (2)$$

$$H + RH \underset{k_{r_3}}{\overset{k_{f_3}}{\rightleftharpoons}} R + H_2 \qquad (3)$$

or

$$H + R + M \underset{k_{r_2}}{\overset{k_{f_2}}{\rightleftharpoons}} RH + M \qquad (2')$$

$$H + RH \underset{k_{r_3}}{\overset{k_{f_3}}{\rightleftharpoons}} R + H_2 \qquad (3')$$

If the reactions above are the dominant paths for the variation of the hydrogen-atom concentration along a nonequilibrium nozzle flow the concentration gradient is given by

$$\begin{aligned} \rho u \frac{d\gamma_H}{dx} = &-2\left(k_{f_1}\rho^3\gamma_H^2\gamma_M - k_{r_1}\rho^2\gamma_{H_2}\gamma_M\right) \\ &-\left(k_{f_2}\rho^2\gamma_H\gamma_R - k_{r_2}\rho\gamma_{RH}\right) \\ &-\left(k_{f_3}\rho^2\gamma_H\gamma_{RH} - k_{r_3}\rho^2\gamma_R\gamma_{H_2}\right) \end{aligned} \qquad (12)$$

Similarly, the rate of production of the stable species in the catalytic mechanism, RH, is given by

$$\begin{aligned} \rho u \frac{d\gamma_{RH}}{dx} = &+\left(k_{f_2}\gamma_H\gamma_R\rho^2 - k_{r_2}\rho\gamma_{RH}\right) \\ &-\left(k_{f_3}\gamma_{RH}\gamma_H\rho^2 - k_{r_3}\rho^2\gamma_R\gamma_{H_2}\right) \end{aligned} \qquad (13)$$

If the alternative path is to be a successful way of enhancing hydrogen-atom recombination, the species RH must be present throughout the expansion in a small, yet finite concentration. This is analogous to the stationary state found for catalysts in nonflowing systems. Thus, assuming $d\gamma_{RH}/dx = 0$ in Eq. (13) and substituting the result in Eq. (12) yields

$$\rho u \frac{d\gamma_H}{dx} = -2\left(k_{f_1} \rho^3 \gamma_H^2 \gamma_M - k_{r_1} \rho^2 \gamma_{H_2} \gamma_M\right)$$

$$-2\left(k_{f_2} \gamma_H \gamma_R \rho^2 - k_{r_3} \rho \gamma_{RH}\right) \tag{14}$$

In a nonequilibrium nozzle flow of a dissociated, diatomic gas, the rate of recombination decreases rapidly as the gas cools in the expansion. Also, it lags behind the value required to maintain chemical equilibrium as the gas expands. Since the rates of the recombination-dissociation reaction decrease as the gas expands, the composition ultimately becomes constant or frozen. Furthermore, since the dissociation rate decreases exponentially with temperature it decreases much more rapidly than the recombination rate. Thus, at some point in the so-called "freezing region" of a nonequilibrium expansion, the reverse rate of a recombination-dissociation reaction becomes negligible compared to the forward rate. When the reverse rates of reactions (1) and (2) become negligible, Eq. (14) may be written

$$\rho u \frac{d\gamma_H}{dx} \simeq -2\left(k_{f_1} \rho^3 \gamma_H^2 \gamma_M + k_{f_2} \gamma_H \gamma_R \rho^2\right) \tag{15}$$

If a lower frozen hydrogen-atom concentration and hence a gain in performance is to be realized in a nozzle expansion then in the freezing region

$$C = \frac{\left(\rho u \frac{d\gamma_H}{dx}\right)_{catalyzed}}{\left(\rho u \frac{d\gamma_H}{dx}\right)_{pure\ H_2}} > 1 \qquad (16)$$

Assuming that $k_{f_1} \rho^3 \gamma_H^2 \gamma_M$ is approximately the same in the catalyzed and uncatalyzed flow, a parameter indicative of the catalysis may be defined

$$C' \cong 1 + \frac{k_{f_2} \gamma_R}{k_{f_1} \rho \gamma_H \gamma_M} \qquad (17)$$

If the first step in Eq. (2) is termolecular as in (2') then

$$C' \cong 1 + \frac{k_{f_2} \gamma_R}{k_{f_1} \gamma_H} \qquad (17')$$

Benson[4] derived an expression similar to Eq. (17') assuming that H_2 is the dominant third body in the termolecular recombination and that $k_{h_2} << k_{f_3} \rho \gamma_H$.

The parameter C is essentially an indication of the inequality in Eq. (16). For a flowing system C varies from point to point in the flow. In order for gas-phase catalysis to be successful, the inequality (16) must hold over a portion of the expansion before freezing occurs. The information available from the catalysis studies using carbon and oxygen addition can be used to evaluate C .

In the numerical solutions for the hydrogen-carbon and hydrogen-oxygen systems, the balance point between catalysis and the molecular-weight penalty has been found by varying the rate constants for the catalytic

mechanisms. The variation of C along the nozzle for this balanced condition is shown in Table 7 for T_o = 4500°K, p_o = 10 atm and O/H and C/H atom ratios of .01. In the above derivation for C the reverse rates of reactions (1) and (2) were neglected. The point in the expansion where this assumption becomes valid and C truly represents $(\rho u d\gamma_H/dx)_{cat.}/(\rho u d\gamma_H/dx)_{H_2}$ is noted in Table 7.

In Table 7 two sets of values are shown for C at each area ratio. One set of values was obtained from the following relations

$$C_{H\text{-}O} = \frac{\left[k_{f_1}\rho^3\gamma_H^2\gamma_{M_1} + k_{f_2}\rho^3\gamma_H^2\gamma_{M_2} + k_{f_3}\rho^3\gamma_H\gamma_{OH}\gamma_{M_3} + k_{f_4}\rho^3\gamma_H\gamma_{OH}\gamma_{M_4} + k_{f_{11}}\rho^3\gamma_H\gamma_O\gamma_{M_{11}}\right]_c}{\left[k_{f_1}\rho^3\gamma_H^3 + k_{f_2}\rho^3\gamma_H^2\gamma_{H_2}\right]_u} \tag{18}$$

$$C_{H\text{-}C} = \frac{\left[k_{f_1}\rho^3\gamma_H^2\gamma_{M_1} + k_{f_2}\rho^3\gamma_H^2\gamma_{M_2} + k_{f_4}\rho^2\gamma_H\gamma_{C_2H}\right]_c}{\left[k_{f_1}\rho^3\gamma_H^3 + k_{f_2}\rho^3\gamma_H^2\gamma_{H_2}\right]_u} \tag{19}$$

where the subscripts c and u denote the catalyzed and uncatalyzed systems. The number subscripts in (18) refer to the reactions listed in Table 1. For the 4 species, 4 reaction hydrogen-carbon model the reaction mechanism was

$$\begin{aligned}
&1.\ H + H + M_1 \overset{k_{f_1}}{\rightleftharpoons} H_2 + M_1 && M_1 = H\\
&2.\ H + H + M_2 \overset{k_{f_2}}{\rightleftharpoons} H_2 + M_2 && M_2 = H_2, C_2H, C_2H_2\\
&3.\ H + C_2H_2 \overset{k_{f_3}}{\rightleftharpoons} C_2H + H_2\\
&4.\ H + C_2H \overset{k_{f_4}}{\rightleftharpoons} C_2H_2
\end{aligned} \tag{20}$$

the number subscripts in (19) refer to these reactions. The second set of values for C shown in Table 7 were obtained using the approximation

$$\left(k_{f_1}\rho^3\gamma_H^2\gamma_{M_1} + k_{f_2}\rho^3\gamma_H^2\gamma_{M_2}\right)_c = \left(k_{f_1}\rho^3\gamma_H^3 + k_{f_2}\rho^3\gamma_H^2\gamma_{H_2}\right)_u \qquad (21)$$

Using Eq. (21), Eqs. (18) and (19) become

$$C_{H\text{-}O} \cong 1 + \left(\frac{k_{f_3}\gamma_{OH}\gamma_{M_3} + k_{f_4}\gamma_{OH}\gamma_{M_4} + k_{r_{11}}\gamma_O\gamma_{M_{11}}}{k_{f_1}\gamma_H\gamma_{M_1} + k_{f_1}\gamma_H\gamma_{M_2}}\right)_c \qquad (18')$$

$$C_{H\text{-}C} \cong 1 + \left(\frac{k_{f_4}\gamma_{C_2H}}{\rho\gamma_H\left[k_{f_1}\gamma_{M_1} + k_{f_2}\gamma_{M_2}\right]}\right)_c \qquad (19')$$

As can be seen from Table 7 the assumption of Eq. (21) is accurate only at the throat. Also, the order of magnitude of the value at the throat is representative of the order of magnitude of C through the freezing region.

As noted in Table 7 the result obtained for the hydrogen-oxygen system using the upper limit of the experimental rates has been taken as the trade-even result. From Table 4 the specific impulse for this mixture is seen to be 1508 sec while the pure hydrogen value is 1503 sec. The trade-even result for the hydrogen-carbon system was found by performing nozzle-flow solutions with the simplified (4 x 4) kinetic model described in Sec. 2. As discussed in Sec. 2 the concentrations of the hydrocarbon species are over-

estimated by about 50% by this model. Thus, the value of C_{H-C} displayed for the hydrogen-carbon system in Table 7 is higher by about a factor of 2 than that obtained using the 8-species, 12-reaction kinetic model.

The (4 x 4) model for the hydrogen-carbon system was employed to obtain additional nozzle-flow solutions for T_0 = 4500°K, p_0 = 10 atm, and a wide variation in the reaction-rate constants for the bimolecular reactions (reactions 3 and 4 in Eq. (20)). The results for the specific impulse are shown in Table 8 together with the values of C_{H-C} evaluated at the throat using Eq. (19'), i.e., also shown in Table 8 is the variation of C_{H-C} along the nozzle for the highest rates used in the calculation. These latter values of C_{H-C} were calculated using Eq. (19) since the approximation made in Eq. (21) is not accurate in the freezing region.

The results shown in Tables 7 and 8 indicate the following. Equations (19) and (19') give the same results for C_{H-C} at the throat. The value calculated at the throat is representative of the order of magnitude of C_{H-C} through the freezing region for the case where a substantial gain in impulse results as well as when the impulse is essentially the pure-hydrogen value. The throat value of C_{H-C} is proportional to the value of k_{f_4}, the forward rate constant in reaction 4 of Eq. (20), for the case where the flow remains near equilibrium at the throat. Hence the increase of impulse due to an increase in C_{H-C} (or k_{f_4}) may be compared with the results shown in Fig. 1 for the dependence of the impulse on the value of the termolecular recombination-rate constant k_{f_1}. Such a comparison for the hydrogen-carbon results of Table 8 indicates that an order of magnitude change in k_{f_4} is slightly more effective than an order-of-magnitude

change in k_{f_1}. This behavior is to be expected because, for the hydrogen-carbon system, both steps in the catalytic mechanism are bimolecular.

The degree to which hydrogen-atom recombination is enhanced by gas-phase catalysis depends on the integral of dr_H/dx along the nozzle. Since this integration cannot be done analytically it is difficult to assess the effectiveness of a given additive without numerical computation. However, since the value of C at the throat is representative of the value through the freezing region this parameter may be used to make a preliminary assessment. For example, suppose the rate constants are well known for a mixture which provides an alternative path for hydrogen-atom recombination. If the termolecular and catalytic paths are the dominant reactions which remove hydrogen atoms, C may be evaluated using the equilibrium throat conditions. Then, if the catalyst RH is stable over the range of conditions in the freezing region and C is appreciably greater than unity a significant percentage of the available gain in impulse can be realized.

The parameter C may also be useful if the rate constants are not well known for a mixture. By varying k_{f_2}, the forward rate constant for the first step in the catalytic recombination path (Eq. (2)), within the expected limits, the range of values of specific impulse possible can be estimated. If the largest expected value of C at the throat is not much larger than unity only marginal gains in impulse can be anticipated.

In the present discussion the question of how large a gain in specific impulse is significant has not been answered. This question is discussed in the ensuing section.

5.2 Implications of Nozzle-Flow Studies to Upper-Stage Rockets

The results of the nozzle-flow solutions for the hydrogen-oxygen and hydrogen-carbon systems indicate that a marginal performance increase relative to pure-hydrogen rocket nozzles is feasible. In this section, it is suggested that even a marginal gain in specific impulse may be important in the application of upper stage rockets. If the same impulse available with pure hydrogen can be obtained with a more dense mixture, a sizable saving in tankage weight may be possible.

For infinite expansion the thrust and specific impulse of a rocket nozzle are given by

$$T = \frac{\dot{m}\, V_{exit}}{g} \tag{22}$$

and

$$I_{sp} = \frac{V_{exit}}{g} = \frac{T}{\dot{m}} \tag{23}$$

where $\dot{m}$ is the mass flow rate, V_{exit} the exit velocity, and g the acceleration of gravity. Suppose that the same specific impulse is available with a pure hydrogen and a hydrogen-plus-catalyst mixture. Also, suppose that a given velocity increment is desired for the rocket stage. Then, by the definition of specific impulse, the same mass of propellant would be required in both cases.

Assume that the mass of propellant required is M. Since the atomic weight of hydrogen is very close to 1 there are M gram-atoms of hydrogen in the pure-hydrogen propellant. If the additive in the hydrogen-plus-

additive propellant contains only one other element besides hydrogen then

$$(n_H)_1 + (n_H)_2 + n_a m_a = M \tag{24}$$

where $(n_H)_1$ is the number of gram-atoms of hydrogen stored as hydrogen, $(n_H)_2$ is the number of gram-atoms of hydrogen stored in the additive, and n_a and m_a are the number of gram-atoms and atomic weight of the other element in the additive. Letting y denote the ratio of gram-atoms of the additive element to the total number of gram-atoms of hydrogen in the mixture

$$y = \frac{n_a}{(n_H)_1 + (n_H)_2} \tag{25}$$

Then, Eq. (24) can be written

$$\left[(n_H)_1 + (n_H)_2\right] (1 + y m_a) = M \tag{26}$$

Further assume that the hydrogen and a stable form of the additive are stored as liquids. In order to have a lower tankage volume for the hydrogen-plus-additive case the specific gravity of the additive must be much larger than that of liquid hydrogen. The percentage decrease in tankage volume η, is given by

$$\eta = \frac{\text{volume of tankage saved}}{\text{volume of tankage for pure hydrogen case}}$$

$$= \frac{\left\{\left[M - (n_H)_1\right] - \left[\frac{M - (n_H)_1}{Z}\right]\right\}}{M}$$

or

$$\eta = \left(1 - \frac{(n_H)_1}{M}\right)\left(1 - \frac{1}{Z}\right) \tag{27}$$

where Z is the ratio of the specific gravity of the additive to that of liquid hydrogen. It should be pointed out that to be consistent with requiring the same velocity increment and the same specific impulse, any saving in tankage weight should be considered to be used for additional payload thereby keeping the total weight of the rocket constant.

If $X_\alpha H_\beta$ is the chemical formula of the form in which the catalyst is stored then, since $n_a/(n_H)_2 = \alpha/\beta$, Eq. (25) yields

$$\frac{1}{y} = \left[1 + \frac{(n_H)_1}{(n_H)_2}\right] \beta/\alpha \tag{28}$$

Now using Eq. (28), Eq. (26) may be written

$$\frac{M}{(n_H)_1} = \left[\frac{1}{1 - \frac{\beta}{\alpha} y}\right]\left(1 + y\, m_\alpha\right) \tag{29}$$

Once the additive and the percentage of the catalyst in the mixture have been chosen, Eqs. (27) and (29) give the percentage saving in tankage volume. From Eq. (29) it can be seen that maximizing β/α (within the restriction of a high specific-gravity fluid) and/or y (the amount of catalyst) increases η , the percentage decrease in tankage volume.

The results of the numerical solutions for the hydrogen-carbon system show that a marginal gain in specific impulse is possible for C/H atom fractions up to .02. Assuming that the specific impulse is the same for the

hydrogen and hydrogen-carbon systems and that the additive is stored as octane (C_8H_{18}), the ratio $M/(n_H)$, and η were computed for $y = .01$ and .02. The results are shown in Table 9. Octane was chosen as the additive in order to store as much hydrogen as possible with the additive and to use an additive which is a liquid of high specific gravity at atmospheric conditions. As seen from Table 9, up to 21% of the tankage volume could be saved by using a hydrogen-carbon propellant as opposed to pure hydrogen.

The recent results obtained for the hydrogen-oxygen system indicate that a marginal gain in impulse could be obtained for an O/H atom fraction up to .01. The above analysis has also been applied to the case of O/H = .01, assuming the additive to be stored as H_2O. The results are also presented in Table 9. For this case 14.6% of the tankage volume can be saved.

On the basis of the above discussion the marginal gains in specific impulse found in the present studies may be quite important for upper-stage, hydrogen rocket engines. Admittedly, the above analysis is idealized. However, the estimates for the performance gain using gas-phase catalysis are conservative. Also, the fact that additives may be chosen that are liquid at ordinary pressure and hence require lighter tankage would compensate for the additional complications of storing two fluids rather than one. Hence, a significant portion of tankage weight might either be saved or converted to payload weight by using gas-phase catalysis.

6. CONCLUSIONS

Numerical solutions have been obtained for rocket-nozzle expansions of hydrogen with trace amounts of oxygen and oxygen-nitrogen additive. The reservoir conditions treated, T_o = 4500°K and p_o = 1.0 atm, 10.0 atm, have application to nuclear or electrically heated upper-stage rockets. As found previously for carbon addition, a slight loss or gain in specific impulse results from oxygen addition, within the scatter in rate-constant data. More accurate rate-constant data would be necessary to arrive at definite conclusions for any additive. Oxygen-nitrogen addition appears to provide no further catalysis than achieved using only oxygen.

The results for the hydrogen-carbon and hydrogen-oxygen systems have been applied to establish the minimum requirements for successful additives. A "catalytic parameter" has been defined which indicates whether or not, and approximately how large a gain in impulse can be expected with a given additive. The numerical results obtained to date have also been used to demonstrate that gas-phase catalysis, although providing marginal gains in impulse, might possibly lead to savings of up to 20% in upper-stage tankage weight.

REFERENCES

1. Sänger-Bredt, I., Astronautica Acta 3, 241 (1957). (Available in English translation as NASA TT F-1).
2. Hall, J. G., Eschenroeder, A. Q., and Klein, J. J., ARS Journal 30, 188 (1960).
3. Eschenroeder, A. Q. and Lordi, J. A., Ninth International Symposium on Combustion, Academic Press, New York, 1963, pp. 241-256. (Also available as CAL Rept. AD-1689-A-1, August 1962).
4. Benson, S. W., J. Chem. Phys. 38, 2285 (1963).
5. Light, J. C. and Schuler, K. E., J. Chem. Phys. 38, 1880 (1963).
6. Duff, R., Private communication.
7. Janaf Thermochemical Tables - published by Dow Chemical Company, Dec. 31, 1960.
8. Bulewicz, E. M. and Sugden, T. M., Proc. Roy. Soc. A, 277, 143 (1964).
9. Ellis, G. E., Marquardt Corp. Rept. MR 20, 202, Nov. 1962.
10. Rink, J. P., J. Chem. Phys. 36, 262-265 (1962).
11. Sutton, E. A., J. Chem. Phys. 36, 2929 (1962).
12. Patch, R. W., J. Chem. Phys. 36, 1919-1924 (1962).
13. Bulewicz, E. M. and Sugden, T. M., Trans. Faraday Soc. 54, 1855 (1958).
14. Schott, G. L., J. Chem. Phys. 32, 710-716 (1960).
15. Fenimore, C. P. and Jones, G. W., J. Phys. Chem. 65, 993 (1961).
16. Kaufman, F. and DelGreco, F. P., Ninth International Symposium on Combustion, Academic Press, New York, 1963, p. 659.

17. Semenov, N., Chemical Kinetics and Chain Reactions, Clarendon Press, Oxford, 1935.

18. Duff, R. E., J. Chem. Phys. 28, 1193-1197 (1958).

19. Wray, K. L., Teare, J. D., Kivel, B., and Hammerling, P., Eighth International Symposium on Combustion, Williams and Wilkins, Baltimore, 1962, pp. 328-339.

20. Wray, K. L. and Teare, J. D., J. Chem. Phys. 36, 2582-2596 (1962).

21. Glick, H. S., Klein, J. J., and Squire, W., J. Chem. Phys. 27, 850-857 (1957).

22. Clyne, M. A. A. and Thrush, B. A., Discussions Faraday Soc. 33, 139 (1962).

23. Fowler, R. G., Proc. of the 1962 Heat Transfer and Fluid Mechanics Institute, Stanford Univ. Press, California, 1962, pp. 279-294.

24. Eschenroeder, A. Q., Boyer, D. W., and Hall, J. G., Phys. Fluids 5, 615 (1962).

25. Mates, R. E. and Lordi, J. A., Aerospace Research Laboratories Rept. ARL 65-2, Jan. 1965.

26. Sutton, G. W., Rocket Propulsion Elements, J. Wiley and Sons, New York, 1958.

27. Handbook of Chemistry and Physics, published by The Chemical Rubber Co., 45th edition, 1964-1965.

Table I

REACTION RATE CONSTANTS FOR HYDROGEN-OXYGEN-NITROGEN SYSTEM

REACTION	THIRD BODY	RATE CONSTANT	SOURCE
1. $H + H + M \rightleftharpoons H_2 + M$	H, H_2O, HNO	$3.5 \times 10^{17}(T)^{-1/2}$	AVERAGE OF VALUES REPORTED BY REFS. 10-12
2. $H + H + M \rightleftharpoons H_2 + M$	$H_2, O_2, O, OH, N, N_2, NO$	$7.0 \times 10^{16}(T)^{-1/2}$	AVERAGE OF VALUES REPORTED BY REFS. 10-12
3. $H + OH + M \rightleftharpoons H_2O + M$	H, OH, H_2O, HNO	$2.2 \times 10^{19}(T)^{-1/2}$	OBTAINED FROM DATA OF REF. 13 AT 1650 K AND M = H_2O. SAME TEMPERATURE DEPENDENCE AND RELATIVE EFFICIENCY OF THIRD BODIES AS k_{f_1} AND k_{f_2} ASSUMED.
4. $H + OH + M \rightleftharpoons H_2O + M$	H_2, O_2, O, N, N_2, NO	$4.4 \times 10^{18}(T)^{-1/2}$	
5. $H_2 + OH \rightleftharpoons H_2O + H$	- - -	$3 \times 10^{14} e^{-6000/R_oT}$	SELECTED VALUE[14] AGREES WELL WITH OTHER RECENTLY REPORTED VALUES[15,16]
6.* $H + O_2 \rightleftharpoons OH + O$	- - -	$3 \times 10^{14} e^{-17,500/R_oT}$	VALUE CHOSEN[14] REPRESENTS AVERAGE OF REPORTED DATA
7. $H_2 + O \rightleftharpoons OH + H$	- - -	$1.2 \times 10^{13} e^{-6000/R_oT}$ $(3 \times 10^{14} e^{-6000/R_oT})$	VALUE CHOSEN[17] IS ABOUT AVERAGE OF REPORTED DATA REF. 18
8. $OH + OH \rightleftharpoons H_2O + O$	- - -	$3 \times 10^{14} e^{-2500/R_oT}$	HIGHEST REPORTED VALUE [18] SELECTED
9.* $H_2 + O_2 \rightleftharpoons OH + OH$	- - -	$10^{14} e^{-118,000/R_oT}$	ONLY VALUE REPORTED[18]
10.* $O_2 + M \rightleftharpoons O + O + M$	ALL SPECIES	$1.19 \times 10^{12}(T)^{-1.5} e^{-118,000/R_oT}$	AVERAGE OF REPORTED VALUES [19]
11. $OH + M \rightleftharpoons O + H + M$	ALL SPECIES	$10^{21}(T)^{-1.5} e^{-101,000/R_oT}$ $(3 \times 10^{21}(T)^{-1.5} e^{-107,000/R_oT})$	VALUE SUGGESTED BY DUFF [18] REF. 23
12. $N_2 + M \rightleftharpoons N + N + M$	ALL SPECIES	$9.9 \times 10^{20}(T)^{-1.5} e^{-225,000/R_oT}$	VALUE CHOSEN [19] MEASURED FOR M = O, O_2, NO AND AGREES WITH OTHER MEASUREMENTS FOR SAME THIRD BODIES[20]
13.* $N_2 + O_2 \rightleftharpoons 2NO$	- - -	$9.1 \times 10^{24}(T)^{-2.5} e^{-128,000/R_oT}$	HIGHEST OF REPORTED VALUES CHOSEN [20]
14. $NO + M \rightleftharpoons N + O + M$	ALL SPECIES	$5.18 \times 10^{21}(T^{-1.5}) e^{-150,000/R_oT}$	OBTAINED FROM $k_{r_{14}}$ REPORTED IN REF. 18
15. $O + N_2 \rightleftharpoons NO + N$	- - -	$5 \times 10^{13} e^{-75,000/R_oT}$	GOOD AGREEMENT AMONG REPORTED VALUES. VALUE CHOSEN FIRST REPORTED IN REF. 21.
16. $O_2 + N \rightleftharpoons NO + O$	- - -	$10^{12}(T)^{1/2} e^{-6,200/R_oT}$	HIGHEST OF REPORTED VALUES [19]
17. $H + NO + M \rightleftharpoons HNO + M$	ALL SPECIES	$2.32 \times 10^{18}(T)^{-.9}$	REF. 22
18. $H + HNO \rightleftharpoons H_2 + NO$	- - -	$1.4 \times 10^{11}(T)^{1/2}$	REF. 8
19. $OH + HNO \rightleftharpoons H_2O + NO$	- - -	$2.1 \times 10^{12}(T)^{1/2}$	$k_{f_{19}}$ TAKEN AS 15 $k_{f_{18}}$ AS SUGGESTED IN REF. 8

Table 2

CONTRIBUTIONS OF INDIVIDUAL REACTIONS TO OVER-ALL SPECIES GRADIENTS IN THE HYDROGEN-OXYGEN SYSTEM

T_o = 4500°K, p_o = 10.0 ATM, O/H = .01

THE QUANTITY $Q_{ij}/\rho u\,(\nu'_{ij} - \nu_{ij})$ IS TABULATED WHERE Q_{ij} IS THE NUMBER OF MOLES OF THE jTH SPECIES PRODUCED BY THE iTH REACTION PER UNIT VOLUME, PER UNIT TIME.

AREA RATIO / REACTION NUMBER	1.01	2.00	4.98	10.0	101.
1	1.6(-2)	9.0(-3)	1.1(-3)	2.6(-3)	3.2(-6)
2	2.2(-3)	1.5(-3)	1.9(-4)	4.4(-5)	5.5(-7)
3	8.4(-3)	4.2(-3)	2.6(-4)	2.2(-5)	2.6(-8)
4	1.1(-3)	7.0(-4)	4.5(-5)	3.8(-6)	4.5(-9)
5	-7.6(-3)	-2.7(-3)	1.3(-3)	6.2(-4)	6.8(-7)
*6	-8.6(-8)	6.8(-7)	4.9(-7)	-1.3(-8)	-1.1(-8)
7	3.7(-4)	4.4(-4)	3.4(-4)	1.7(-4)	3.0(-7)
8	-3.6(-4)	-2.9(-4)	-9.0(-5)	-1.4(-5)	3.0(-9)
*9	6.7(-9)	1.5(-9)	1.9(-11)	5.6(-14)	-4.6(-32)
*10	-6.6(-8)	-2.4(-8)	-1.8(-9)	-3.0(-10)	-1.0(-11)
11	-1.0(-4)	-5.5(-5)	-7.0(-6)	-1.8(-6)	-1.4(-7)

*REACTIONS FOUND TO HAVE NEGLIGIBLE EFFECT ON CHEMICAL KINETIC DESCRIPTION OF SPECIES H_2, H, O, OH, H_2O.

NUMBERS IN PARENTHESES INDICATE POWERS OF 10.

Table 3

EFFECT OF RATE-CONSTANTS FOR CATALYTIC MECHANISM ON HYDROGEN-CARBON AND HYDROGEN-OXYGEN FLOWS

(T_o = 4500°K, p_o = 10.0 atm.)

GAS MIXTURE	FROZEN H-ATOM CONCENTRATION (MOLES/GM OF MIXTURE)	I_∞ (SECS.)	RATE CONSTANTS
PURE HYDROGEN	.3625	1503	
HYDROGEN-OXYGEN (O/H = .01)	.3057	1423	PREFERRED VALUES USED FOR ALL REACTIONS.
HYDROGEN-OXYGEN (O/H = .01)	.2511	1508	HIGHEST VALUES LISTED IN TABLE I USED FOR REACTIONS 7 AND 11.
HYDROGEN-CARBON (C/H = .01)	.2999	1473	LOWEST VALUES USED IN BIMOLECULAR REACTIONS.[3]
HYDROGEN-CARBON (C/H = .01)	.2107	1605	HIGHEST VALUES USED IN BIMOLECULAR REACTIONS.[3]

Table 4

CONTRIBUTIONS OF INDIVIDUAL REACTIONS TO THE HYDROGEN-ATOM GRADIENT IN THE HYDROGEN-OXYGEN SYSTEM (T_o = 4500°K, p_o = 10 ATM, O/H = .01)

CASE I PREFERRED VALUES USED FOR REACTIONS LISTED IN TABLE I.

AREA RATIO / REACTION NO.	1.01	2.0	5.0	10.
1	-3.2(-2)	-1.8(-2)	-2.1(-3)	-5.2(-4)
2	-4.4(-3)	-3.0(-3)	-3.8(-4)	-8.8(-5)
3	-8.4(-3)	-4.2(-3)	-2.6(-4)	-2.2(-5)
4	-1.1(-3)	-7.0(-4)	-4.5(-5)	-3.8(-6)
5	-7.6(-3)	-2.7(-3)	+1.3(-3)	+6.2(-4)
7	+3.7(-4)	+4.4(-4)	+3.4(-4)	+1.7(-4)
11	-1.0(-4)	-5.5(-5)	-7.0(-6)	-1.8(-6)

CASE II HIGHEST VALUES USED FOR REACTION 7 AND 11 LISTED IN TABLE I.

AREA RATIO / REACTION NO.	1.01	2.0	5.0	10.
1	-5.8(-3)	-3.2(-3)	-9.8(-4)	-2.4(-4)
2	-7.8(-4)	-6.0(-4)	-2.2(-4)	-5.6(-5)
3	-1.6(-3)	-8.5(-4)	-2.1(-4)	-3.1(-5)
4	-2.0(-4)	-1.5(-4)	-4.7(-5)	-7.1(-6)
5	-1.1(-5)	-9.5(-3)	-6.7(-4)	+8.4(-4)
7	-3.0(-2)	-2.8(-2)	-7.7(-3)	-7.3(-4)
11	-3.1(-2)	-3.5(-2)	-7.4(-3)	-1.0(-3)

NUMBERS IN PARENTHESES INDICATE POWERS OF 10.

Table 5

EFFECT OF RESERVOIR PRESSURE ON PERFORMANCE OF HYDROGEN-OXYGEN AND HYDROGEN-CARBON SYSTEMS FOR T_o = 4500°K

GAS MIXTURE	P_o (ATM)	$(\gamma_H)_{FROZEN}$ (MOLES/GM OF MIXTURE)	I_∞ (SECS)
PURE HYDROGEN	10.0	.3625	1503
	1.0	.8188	1435
*HYDROGEN-OXYGEN	10.0	.2511	1508
(O/H = .01)	1.0	.6528	1473
**HYDROGEN-CARBON	10.0	.2107	1605
(C/H = .01)	1.0	.6455	1501

*HIGHEST VALUES OF RATE CONSTANTS LISTED IN TABLE I FOR REACTIONS 7 AND 11.

**HIGHEST VALUES EMPLOYED IN REF. 3 FOR RATE CONSTANTS OF BIMOLECULAR REACTIONS.

TABLE 6

EFFECT OF MIXTURE RATIO ON PERFORMANCE OF HYDROGEN-OXYGEN SYSTEM FOR T_o = 4500°K, p_o = 10 ATM.

O/H	$(\gamma_H)_{FROZEN}$ (MOLES/GM OF MIXTURE)	I_∞ (SECS)
0	.3625	1503
.002	.3174	1535
.005	.2834	1536
.01	.2511	1508
.02	.2115	1347

NOTE: THESE RESULTS WERE OBTAINED USING THE HIGHEST VALUES LISTED IN TABLE I FOR THE RATE CONSTANTS OF REACTIONS 7 AND 11.

Table 7

VARIATION OF CATALYTIC PARAMETER, C, ALONG THE NOZZLE FOR THE HYDROGEN-OXYGEN AND HYDROGEN-CARBON FLOWS HAVING THE SAME IMPULSE AS PURE HYDROGEN

(T_o = 4500°K, p_o = 10 atm.)

AREA RATIO	1.00	1.85	5.29*	11.4*	22.1*
**HYDROGEN-OXYGEN (O/H = .01)					
C (EQ.(18))	2.24	1.24	0.66	0.50	0.41
C (EQ. (18'))	2.29	1.63	1.44	1.22	1.09
AREA RATIO	1.00	1.91	5.22*	11.3*	22.2*
***HYDROGEN-CARBON (C/H = .01)					
C (EQ. (19))	9.64	16.5	7.33	3.52	1.83
C (EQ. (19'))	9.75	23.3	12.2	6.90	3.94

* AREA RATIOS FOR WHICH THE REVERSE RATES IN TERMOLECULAR REACTION AND FIRST REACTION IN CATALYTIC PATH ARE NEGLIGIBLE. ($\frac{R_r}{R_f} < 0.1$)

** THE BALANCE POINT BETWEEN CATALYSIS AND MOLECULAR WEIGHT PENALTY OCCURS WHEN THE HIGH VALUES OF THE RATE CONSTANTS FOR REACTION 7 AND 11 ARE USED IN THE HYDROGEN-OXYGEN CALCULATIONS.

*** THE BALANCE POINT BETWEEN CATALYSIS AND MOLECULAR WEIGHT PENALTY OCCURS WHEN A STERIC FACTOR OF .05 IS USED IN THE REACTIONS INVOLVING ACETYLENE. THIS VALUE IS MIDWAY BETWEEN THE VARIATION CONSIDERED IN REF. 3.

Table 8a

EFFECT OF VARIATION IN BIMOLECULAR RATE CONSTANTS ON THROAT VALUE OF THE CATALYTIC PARAMETER FOR THE HYDROGEN-CARBON SYSTEM (T_o = 4500°K, p_o = 10 ATM., C/H = .01

BIMOLECULAR RATE CONSTANT	CHEMICAL KINETIC MODEL	$(\gamma'_H)_{FROZEN}$ (MOLES/GM OF MIXTURE)	I_∞ (SECS)	C (EQ. (19))
$4.5 \times 10^{10} T^{1/2}$	4 SPECIES, 4 REACTIONS	.3162	1443	1.44
$4.5 \times 10^{11} T^{1/2}$	4 SPECIES, 4 REACTIONS	.2999	1473	5.85
$9.0 \times 10^{11} T^{1/2}$	4 SPECIES, 4 REACTIONS	.2741	1508	9.75
$4.5 \times 10^{12} T^{1/2}$	4 SPECIES, 4 REACTIONS	.2107	1605	44.7
$4.5 \times 10^{13} T^{1/2}$	4 SPECIES, 4 REACTIONS	.1063	1740	438
$4.5 \times 10^{12} T^{1/2}$	8 SPECIES, 12 REACTIONS	.2107	1605	25.2

Table 8b

VARIATION OF THE CATALYTIC PARAMETER ALONG THE NOZZLE FOR THE HIGHEST BIMOLECULAR RATE CONSTANTS SHOWN IN TABLE 8a

AREA RATIO	C (EQ. (19))
1.00	434
1.85	1220
5.29	2150
11.4	2410
22.1	2340

Table 9

PERCENTAGE SAVING IN TANKAGE VOLUME FOR CATALYZED HYDROGEN ROCKET-NOZZLE FLOWS

ADDITIVE	ATOM FRACTION OF ADDITIVE (y)	SPECIFIC GRAVITY[27]	$\frac{M}{(n_H)_1}$ (EQ. (29))	η (EQ. (27))
OCTANE (C_8H_{18})	.01	.7025	1.147	11.5%
OCTANE (C_8H_{18})	.02	.7025	1.30	20.8%
WATER (H_2O)	.01	1.0	1.183	14.6%

SPECIFIC GRAVITY OF LIQUID HYDROGEN - .07. [26]

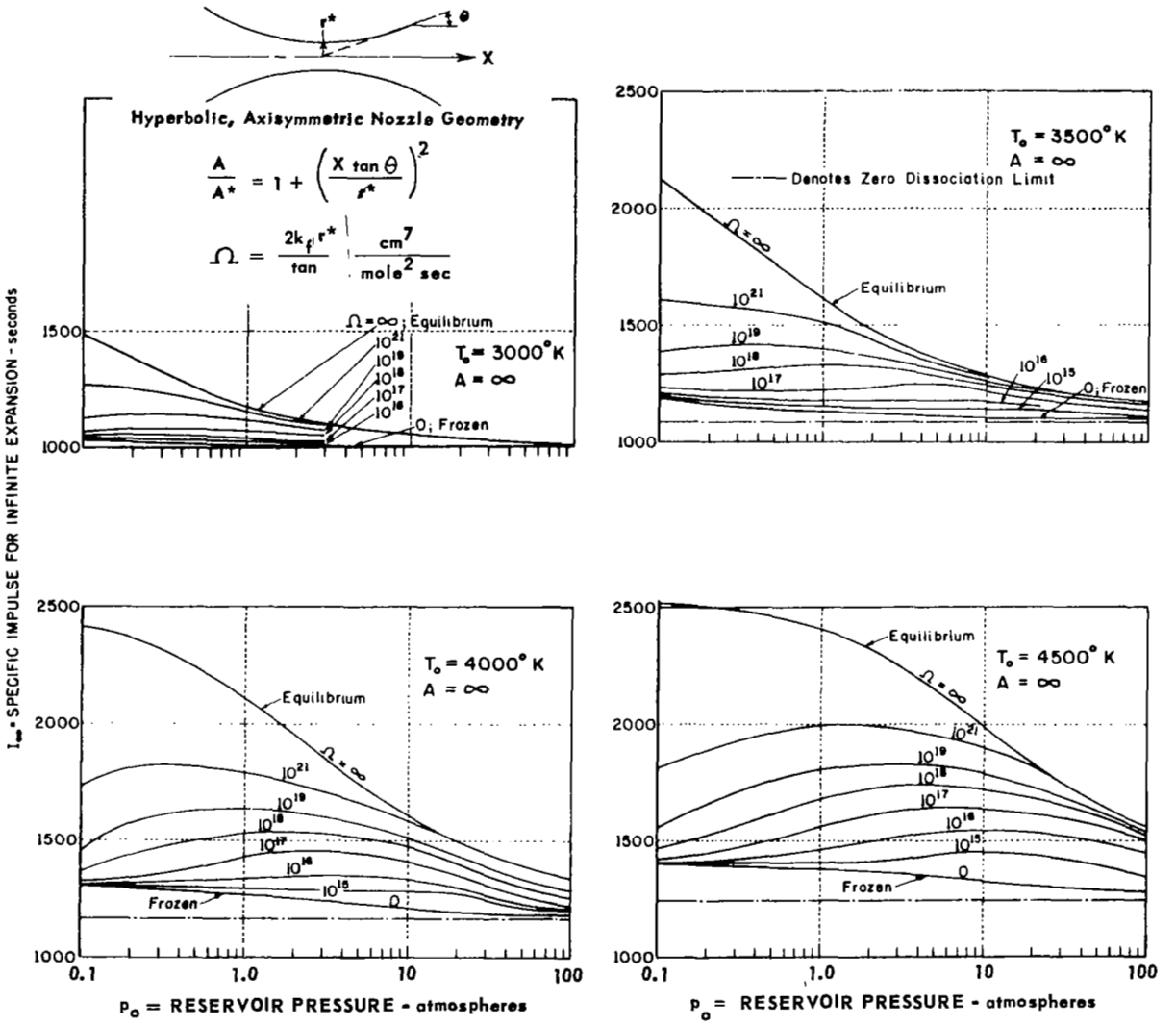

Figure 1 THE INFLUENCE OF CHEMICAL NONEQUILIBRIUM ON THE SPECIFIC IMPULSE OF A HYDROGEN ROCKET NOZZLE WITH INFINITE EXPANSION (TAKEN FROM REF. 2)

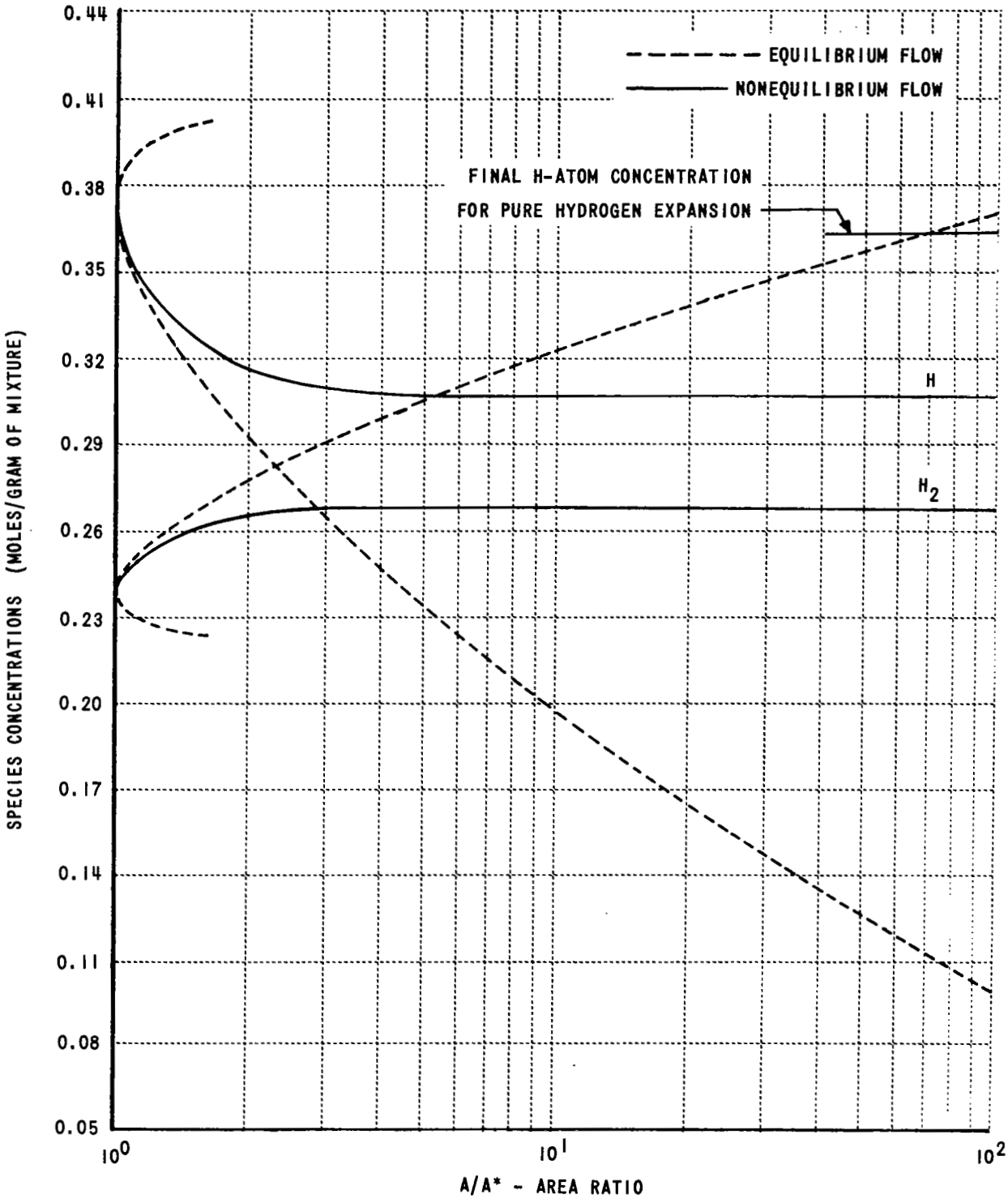

Figure 2a VARIATION OF SPECIES CONCENTRATIONS ALONG HYDROGEN - OXYGEN EXPANSION (T_o = 4500°K, p_o = 10 ATM, O/H = .01)

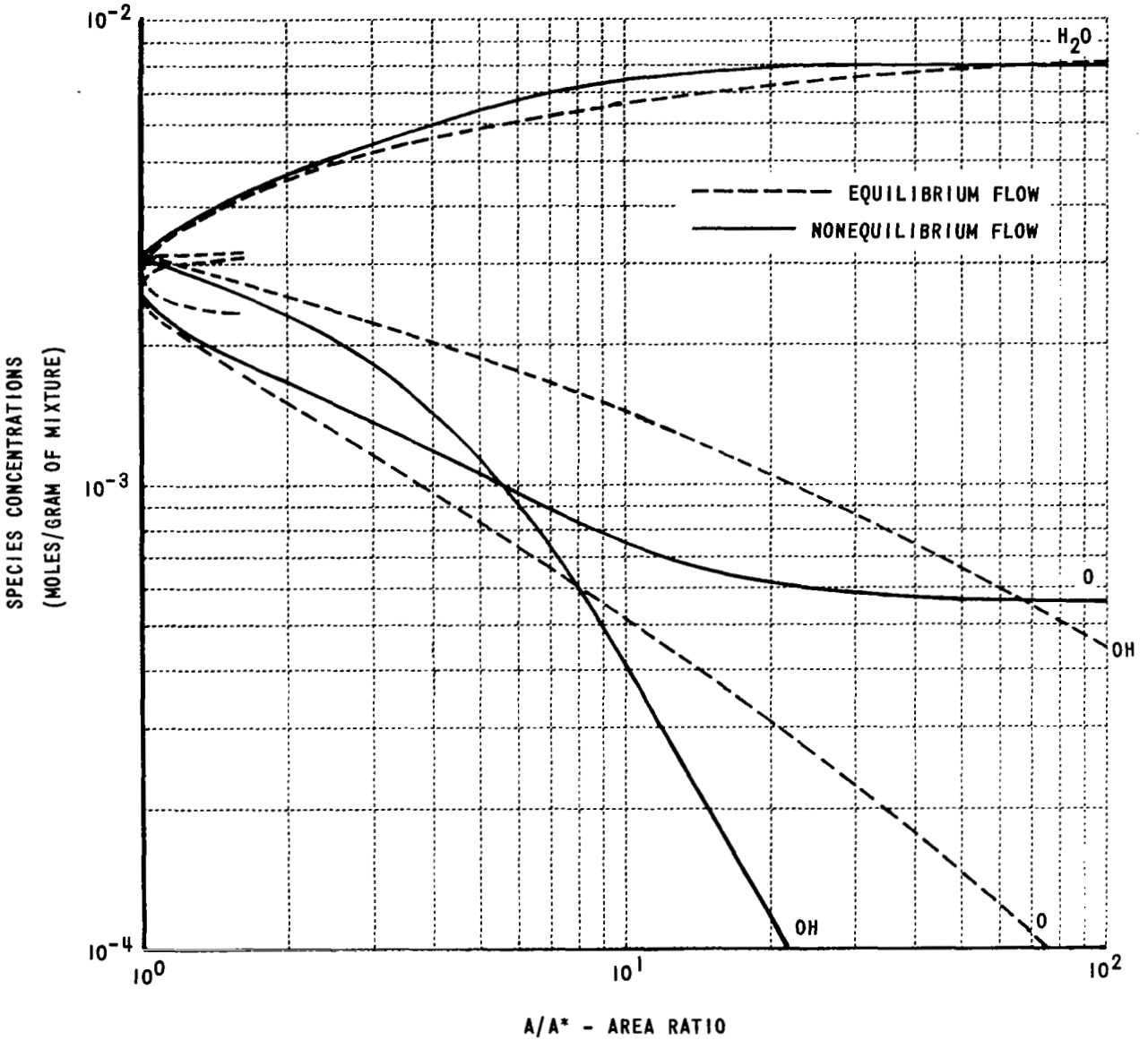

Figure 2b VARIATION OF SPECIES CONCENTRATIONS ALONG HYDROGEN - OXYGEN EXPANSION
(T_o = 4500°K, p_o = 10 ATM, O/H = .01)